Structure of peptidoglycan from Thermus thermophilus HB8.

J C Quintela, E Pittenauer, G Allmaier, V Arán and M A de Pedro
J. Bacteriol. **1995, 177(17):4947.**

JOURNAL OF BACTERIOLOGY, Sept. 1995, p. 4947–4962
0021-9193/95/$04.00+0

Vol. 177, No. 17

Structure of Peptidoglycan from *Thermus thermophilus* HB8

JOSÉ CARLOS QUINTELA,[1] ERNST PITTENAUER,[2] GÜNTER ALLMAIER,[2]
VICENTE ARÁN,[3] AND MIGUEL A. DE PEDRO[1]*

Centro de Biología Molecular "Severo Ochoa" Consejo Superior de Investigaciones Científicas-Universidad Autónoma de Madrid, Facultad de Ciencias, Campus de Cantoblanco, 28049 Madrid,[1] and Instituto de Química Médica, Consejo Superior de Investigaciones Científicas, 28006 Madrid,[3] Spain, and Institute of Analytical Chemistry, University of Vienna, A-1090 Vienna, Austria[2]

Received 13 April 1995/Accepted 27 June 1995

The composition and structure of peptidoglycan (murein) extracted from the extreme thermophilic eubacterium *Thermus thermophilus* HB8 are presented. The structure of 29 muropeptides, accounting for more than 85% of total murein, is reported. The basic monomeric subunit consists of *N*-acetylglucosamine–*N*-acetylmuramic acid–L-Ala–D-Glu–L-Orn–D-Ala–D-Ala, acylated at the δ-NH_2 group of Orn by a Gly-Gly dipeptide. In a significant proportion (about 23%) of total muropeptides, the N-terminal Gly is substituted by a residue of phenylacetic acid. This is the first time phenylacetic acid is described as a component of bacterial murein. Possible implications for murein physiology and biosynthesis are discussed. Murein cross-linking is mediated by D-Ala–Gly–Gly peptide cross-bridges. Glycan chains are apparently terminated by (1→6)anhydro *N*-acetylmuramic acid residues. Neither reducing sugars nor murein-bound macromolecules were detected. Murein from *T. thermophilus* presents an intermediate complexity between those of gram-positive and gram-negative organisms. The murein composition and peptide cross-bridges of *T. thermophilus* are typical for a gram-positive bacterium. However, the murein content, degree of cross-linkage, and glycan chain length for *T. thermophilus* are closer to those for gram-negative organisms and could explain the gram-negative character of *Thermus* spp.

Thermophilic eubacteria of the genus *Thermus* are receiving considerable attention for their biotechnological potential. They are important sources for thermostable enzymes and are appropriate organisms for genetic engineering and manipulation of genes from reluctant thermophiles (4, 32, 33). *Thermus thermophilus* is delimited by a complex cell envelope (7, 12, 42). This bacterium grows as slender, flexible rods, rather variable in length, that are negative for the Gram reaction (8). Electron microscopy of thin-sectioned specimens shows a multilayered organization of the cell envelope. A thin peptidoglycan (synonym: murein) layer is revealed to be sandwiched between the cytoplasmic membrane and a thick layer (~30 nm) of amorphous material. A protein S-layer masked by amorphous material forms the outermost layer of the cell envelope (7, 12). The S-layer and the murein sacculus interact with each other in spite of the intermediate amorphous layer. The S-layer monomeric protein (P_{100}) can be extracted from cell envelope preparations by Triton X-100 only when murein has been previously degraded. Otherwise, P_{100} remains in the insoluble, murein-containing fraction (19). Furthermore, murein has a strong influence on the crystallographic characteristics of P_{100} planar arrays (12, 13). The S-layer–murein interaction seems to be also important on physiological terms. S-layers are often dispensable (37). However, S-layer-deficient mutants of *T. thermophilus* are seriously impaired in growth and morphology (32). The morphogenetic involvement of the *T. thermophilus* S-layer could be related to unusual properties of the murein sacculus, perhaps forced by adaptation to thermophilic conditions.

The application of high-performance liquid chromatography (HPLC) and mass spectrometry (MS) techniques (1, 22, 45) made it possible to investigate the muropeptide composition of mureins from a small number of sources in the last few years (9, 14, 20, 23, 46, 48, 58). Substantial structural information can be derived from muropeptide composition data (10, 14, 23, 44). Nevertheless, methodology is still far from routine. Murein from *Escherichia coli*, the best known example, yields 50 to 60 peaks upon HPLC, of which about 40 have been fully characterized (22, 23).

The prospect of structural analysis of *T. thermophilus* murein was particularly appealing. Murein properties of extreme thermophilic eubacteria have not been studied in depth yet. However, specific adaptations are likely, as has been demonstrated for other cell envelope constituents (7, 18, 41). The apparent interaction between murein and the S-layer is indicative of peculiarities in the organization of the cell wall that are required for proper morphogenesis.

Early studies of the murein composition of *T. thermophilus* revealed the presence of Ala, Glu, Gly, and Orn in addition to *N*-acetylglucosamine (GlcNAc) and *N*-acetylmuramic acid (MurNAc). Diaminopimelic acid, the canonical diamino acid in gram-negative cell walls, was not detected (42, 53). Therefore, the murein sacculus of *T. thermophilus* was likely to be one of the rare exceptions to the rule for gram-negative bacteria (31, 53). Murein from *T. thermophilus* is also interesting from a methodological point of view. Existing data suggest a degree of structural complexity intermediate between the complexities of gram-positive and other gram-negative bacteria (7, 42) which seems adequate to evaluate the capacities of available analytical methodologies. A better knowledge of murein structure should facilitate further advancements in the elucidation of the structure of the *Thermus* spp. cell envelope and its involvement in the adaptation to life at high temperatures.

MATERIALS AND METHODS

Bacterial strains and growth conditions. *T. thermophilus* HB8 (ATCC 27634) (40) and *E. coli* MC6RP1 (K-12, F^- *proA leuA thr dra drm lysA thi*) (47) were the bacterial strains used throughout this work. The cultivation of *T. thermophilus* was performed in a 20-liter fermentor (Biostat-UD; B. Braun Biotech International GmbH, Melsungen, Germany) at 75°C under strong aeration in a medium

* Corresponding author. Phone: (1) 3978083. Fax: (1) 3974799. Electronic mail address: madepedro@mvax.cbm.uam.es.

consisting of 4 g of yeast extract per liter, 8 g of Bacto Peptone per liter, and 3 g of NaCl per liter (pH 7.5) (32). Cultures of *E. coli* were grown in flasks containing Luria-Bertani medium (34) at 37°C, under vigorous aeration. Growth was monitored by measuring the optical densities of the cultures at 550 nm.

Murein extraction and muramidase digestion. Murein was extracted in the boiling sodium dodecyl sulfate (SDS)-insoluble fraction as described previously (22, 23, 44). To remove colored contaminants, possibly carotenoids, the murein fraction was resuspended in 4% SDS, incubated in a boiling water bath for 1 h, and sedimented by centrifugation (three cycles of 150,000 × *g*, 1 h, 30°C). The murein was washed until it was free of SDS and was further processed for muramidase digestion with Cellosyl (Hoechst, Frankfurt, Germany) as described previously (22, 23). The reaction was stopped by incubating the samples for 5 min in a boiling water bath. Insoluble material was removed by centrifugation (10,000 × *g*, 10 min). Muropeptides were reduced with NaH_4B and kept frozen at −70°C or were immediately subjected to further treatments.

Quantification of diamino acids in murein samples. Murein and muropeptide concentrations were routinely calculated from the diamino acid content. Samples were hydrolyzed in 6 N HCl (12 h, 105°C), vacuum dried, and resuspended in an appropriate volume of distilled water, and the concentration of Orn or *meso*-diaminopimelic acid was quantified by the ninhydrin assay as described previously (61).

Quantification of reducing sugars in murein fractions. The amount of reducing sugars in murein was estimated as described by Ghuysen et al. (21). Murein samples (1 mg of Orn) were divided into two aliquots. One of them was digested to completion with muramidase (Cellosyl) (20 μg/ml, 12 h, 37°C in 50 mM sodium phosphate buffer, pH 4.9) to release muropeptides with reducing MurNAc residues. The reducing power was measured for each sample following color formation at 690 nm, and the proportion of reducing sugars in each aliquot was calculated.

Galactosylation of murein. The galactosylation of terminal GlcNAc residues of murein glycan chains was performed as previously described (3, 52). Triplicate samples of murein (60 nmol of diamino acid) were incubated with milk galactosyltransferase (0.2 U) in the presence of 20 μg of α-lactalbumin–UDP–[^{3}H] galactose (1 mM, 100 μCi/μmol) in a total volume of 100 μl of 10 mM $MnCl_2$–50 mM MOPS (morpholinepropanesulfonic acid) buffer, pH 7.4, for 2 h at 37°C. The reaction was stopped by incubating samples 1 min at 90°C, and a known amount (0.3 mg of diamino acid) of unlabeled murein was then added to each sample. Samples were repeatedly centrifuged (300,000 × *g*, 15 min) and resuspended in water, until no radioactivity (<500 cpm/ml) was detectable in the supernatant. Pellets were then resuspended in water, hydrolyzed in 6 N HCl (12 h, 100°C), vacuum dried, resuspended in an appropriate volume of distilled water, and divided into two equal parts. One part was used to measure incorporated radioactivity by liquid scintillation, while the second part was further processed to measure diamino acid concentration as described above. The comparison of the initial and final murein concentrations allowed the correction for loss during processing.

HPLC analysis of murein composition and muropeptide purification. Muramidase-digested samples were analyzed by HPLC according to the method of Glauner et al. (23) on a Hypersil RP18 column (250 by 4 mm, 3-μm diameter [particle size]; Teknochroma, Barcelona, Spain). Elution buffers were 50 mM sodium phosphate, pH 4.35 (A), and 15% (vol/vol) methanol in 75 mM sodium phosphate, pH 4.95 (B). Elution conditions were as follows: 7 min of isocratic elution in buffer A, 115 min of linear gradient to 100% of buffer B, 50 min of isocratic elution in buffer B. The flow rate was 0.5 ml/min, and the column temperature was 40°C. Muropeptides were collected at the detector outlet, vacuum dried, resuspended in water, and desalted by HPLC as described previously (10). For MS analysis, muropeptides were further purified as indicated below.

Dinitrophenylation and amino acid analysis. Samples of purified muropeptides were dinitrophenylated as previously described (10). Aliquots of murein and native or dinitrophenylated muropeptides were hydrolyzed in 6 N HCl (12 h, 100°C), derivatized with *O*-phthaldialdehyde (OPA), and subjected to amino acid analysis by HPLC as reported previously (10).

Partial acid hydrolysis and peptide analysis of murein and muropeptides. Murein or muropeptide samples (20 to 30 μg of Orn) were hydrolyzed in 2 N HCl for 1 h at 80°C. Hydrolysates were vacuum dried, resuspended in water, OPA derivatized, and analyzed by HPLC on a Hypersil RP18 column (250 by 4 mm; particle size, 3 μm) with commercial peptides as reference compounds. Elution buffers were tetrahydrofurane–methanol–50 mM Na_2HPO_4 plus 50 mM sodium acetate (pH 7.5) (2:2:96) (buffer A) and 65% (vol/vol) methanol (buffer B). The elution conditions were as follows: 8 min of isocratic elution in buffer A, 7 min of linear gradient to 60% of buffer A and 40% of buffer B, 30 min of isocratic elution in 60% buffer A and 40% buffer B, and 75 min of linear gradient to 100% of buffer B. The flow rate was 0.5 ml/min, and the eluate was monitored at 365 nm.

Affinity chromatography on vancomycin-Sepharose. Vancomycin-Sepharose was prepared as described before (15). Muropeptides with D-Ala–D-Ala C-terminal dipeptides are specifically retained and elute only at high pHs, while other muropeptides are readily washed out of the column. A muramidase-digested murein sample containing 0.5 mg of Orn in 1 ml of 20 mM Tris-HCl, pH 7.0, was loaded onto a vancomycin-Sepharose column (matrix bed volume, 1.8 ml) equilibrated in 20 mM Tris-HCl, pH 7.0, buffer. The column was washed with 7 ml of water and then was eluted stepwise with equal volumes (7 ml) of $OH(NH_4)$ solutions adjusted to pH 9, 10, and 11. Eluted fractions were collected, vacuum dried, resuspended in 50 mM sodium phosphate (pH 4.35), and subjected to HPLC analysis as described for muropeptide analysis.

Enzymatic modification of murein-derived amino acids. Conversion of Orn into citrulline by L-ornithine carbamyltransferase was assayed as described previously (38, 43). A sample of murein (100 μg of Orn) was digested with muramidase, and the solubilized muropeptide mixture was subjected to acid hydrolysis (6 N HCl, 12 h, 105°C). The hydrolysate was dried and resuspended in water. Aliquots (containing 25 μg of Orn) of the hydrolysate were treated with 3 U of enzyme (620 U/mg of protein) in 50 mM Tris-HCl buffer, pH 8.5, in a total volume of 100 μl, for 1 h at 37°C. The reaction was stopped by heating the samples to 90°C for 1 min. Protein was precipitated by mixing the samples 1:2 with cold (−20°C) acetone. After 5 min, the samples were centrifuged (10,000 × *g*, 10 min) and supernatants were vacuum dried, resuspended in 250 mM sodium borate buffer, pH 10, and derivatized with OPA. The conversion of Orn into citrulline was assessed by HPLC as described for amino acid analysis.

Conversion of Glu into γ-aminobutyric acid by L-glutamic decarboxylase was assayed as reported previously (25). Aliquots from the same muropeptide hydrolysate as above, or from a solution of L-Glu containing 20 μg of Glu, were incubated with 3 U of L-glutamic decarboxylase (21.3 U/mg of protein) and 50 mM phosphate buffer, pH 5.0, in a total volume of 100 μl, for 1 h at 37°C. The reaction was stopped, and samples were further processed as described above to measure Glu and γ-aminobutyric acid in the reaction mixtures by HPLC.

Conversion of Ala into pyruvate by L-amino acid oxidase was assayed as reported previously (39). A sample (20 μg of Orn) of a purified muropeptide was hydrolized as described above. The hydrolysate was dissolved in water and digested with 0.5 U of L-amino acid oxidase (1.6 U/mg of protein) in 0.3 mM EDTA–50 mM phosphate buffer, pH 7.9, in a total volume of 100 μl, for 1 h at 37°C. The reaction was stopped, and the amount of residual Ala was determined by HPLC as described above.

Enzyme activity units were defined in all instances as the amount of enzyme required to convert 1 μmol of substrate per min under the conditions described above.

Preparation of muropeptides for MS. Desalting and final purification of the collected fractions for mass spectrometric analysis were performed on an HP 1090 high-performance liquid chromatograph or an ABI 172 microliquid chromatograph with an octyldecyl silane Hypersil column (Shandon Scientific) (particle size, 3.5 μm; pore size, 120 Å [12 nm]; column dimensions, 250 by 4 mm or 100 by 2.1 mm). The solvent gradient used was linear from 100% ultrapure water (18 $M\Omega^{-1}$ cm^{-1}), generated by an Elgastat apparatus (Elga) and containing 0.05% trifluoroacetic acid, to 40% acetonitrile, containing 0.035% trifluoroacetic acid, from 5 to 45 min. The flow rate was 1 ml/min for the standard column or 0.1 ml/min for the liquid chromatography microcolumn. The column temperature was maintained at 30°C, and the UV absorbance detector was operated at 210 nm.

MS of muropeptides. Positive and negative ion ^{252}californium plasma desorption (PD) mass spectra were obtained with a Biolon 20 time-of-flight mass spectrometer under the following conditions: length of drift region, 141 mm; accelerating voltage, 17 to 20 kV (positive ion detection) and 15 kV (negative ion detection); time resolution, 1 ns per channel; spectrum accumulation time, 2×10^6 to 5×10^6 fission events (positive ion mass spectra) or 5×10^6 to 1×10^7 (negative ion mass spectra). Mass calibrations were based on H^+ and Na^+ ions for positive ion PD mass spectra and on H^- and CN^- ions for negative ion PD mass spectra. All muropeptides were dissolved in 2 to 5 μl of 0.1% trifluoroacetic acid and were deposited onto nitrocellulose-covered targets (50). After positive and negative ion MS measurement, our previously described nitrocellulose sandwich technique (1) for removing alkali contaminants without sample loss was applied to enhance protonated and deprotonated molecular ion yields.

Positive ion electrospray ionization (ESI) mass spectra were acquired on a Perkin Elmer Sciex API-III triple quadrupole mass spectrometer fitted with an articulated, pneumatically assisted nebulization probe and an atmospheric pressure ionization source. The tuning and calibration solution consisted of a mixture of polypropylene glycols 425, 1000, and 2000 (3.3×10^{-5}, 1×10^{-4}, and 2×10^{-4} M, respectively) in water-methanol-formic acid (50:50:0.1, vol/vol/vol) containing 1 mM ammonium acetate. Purified peptidoglycan monomer samples were dissolved in acetonitrile-water (1:1, vol/vol) containing 0.1% trifluoroacetic acid. Direct infusion of the sample solution into the electrospray chamber was performed with a syringe pump at a flow rate of 3 μl/min. The ion spray source was operated in the positive ion mode at a sampling-orifice potential of 65 V. High-purity air served as the nebulizing gas and was kept at an operating pressure of 250 kPa. Nitrogen gas (99.999%) was used as the curtain gas at a constant flow of 0.8 liter/min. For collision-induced dissociation (CID) tandem MS experiments, precursor ion selection was performed at unit resolution. Precursor ions were selectively transmitted by the first quadrupole mass analyzer and directed into the radio frequency-only quadrupole collision cell containing argon gas. The collision gas thickness was maintained at 7×10^{14} molecules cm^{-2}, and the selected collision energy was 250 eV (laboratory frame of reference). CID spectra were obtained after collision by scanning the second quadrupole mass analyzer to record the fragment ion products. The CID spectrum (see Fig. 3) represents the average of 12 scans obtained with a scan time of 3.88 s across the *m/z* range 100 to 1,200.

Chemical modification of phenylacetic acid. Samples of commercial and murein-derived phenylacetic acid were chemically treated to obtain phenylacetamide, *N*-methyl-phenylacetamide and methylphenyl acetate. Samples of 100 μg of phenylacetic acid were dissolved in 1 ml of Cl_2SO and were kept under reflux for 3 h, and then Cl_2SO was removed by evaporation under vacuum. The residual material was mixed with 1-ml solutions of 25% $OH(NH_4)$, 40% CH_3NH_2, or CH_3OH and allowed to react for 1 h at room temperature. In the first two cases, the mixtures were extracted with chloroform, the organic phase was washed with water and dried with Na_2SO_4, and chloroform was evaporated. In the third case, methanol was evaporated, and the residue was dissolved in 50 mM $NaHCO_3$ and extracted with chloroform. The organic phase was dried with Na_2SO_4, and chloroform was evaporated. The derivatives were then dissolved in 10% acetonitrile in water and analyzed by HPLC (Hypersil RP18 column; 250 by 4 mm; particle size, 3 μm). Chromatography was performed at a flow rate of 0.5 ml/ml under isocratic conditions in 15% acetonitrile for phenylacetamide and *N*-methyl-phenylacetamide (retention times [RTs], 18 and 24 min, respectively) or in 30% acetonitrile for methyl ester (RT, 46 min). Elution was monitored by measuring the A_{258} of the eluate.

Enzymes, chemicals, and radioactive products. Enzymes were purchased from Sigma-Aldrich Química S.A. (Alcobendas, Spain) and E. Merck (Darmstadt, Germany). Radioactive products were from Amersham Iberica (Madrid, Spain). Solvents for HPLC were of the highest grades from E. Merck and Scharlau S.A. (Barcelona, Spain). Products for bacterial growth media were from Difco Laboratories (Detroit, Mich.), and general chemicals were from E. Merck, Sigma, and Scharlau.

RESULTS

Murein content of *T. thermophilus*. Electron microscopy revealed a thin murein layer in the cell envelope of *T. thermophilus* (7, 32). However, no quantitative data were available. Therefore the amount of murein per dry weight unit was determined by chemical quantification of Orn in samples of murein purified from a known amount of cells. The result, 14 μmol of Orn per g (dry weight), is roughly one-half the amount of *meso*-diaminopimelic acid (27 μmol/g) measured in *E. coli* cells in a parallel experiment.

Murein from *T. thermophilus* HB8 is quantitatively solubilized by muramidase digestion. Application of the normal murein purification method to *T. thermophilus* HB8 yielded a fraction which still contained considerable amounts of muramidase-resistant, insoluble material. Incomplete solubilization of murein would call any subsequent analysis into serious question. To investigate solubilization, the amount of Orn, a component likely to be exclusive of murein, was measured in total, muramidase-solubilized, and muramidase-resistant fractions. Fractions were subjected to acid hydrolysis, OPA derivatization, and HPLC analysis. At least 97% of total Orn was recovered in the muramidase-solubilized fraction. Aspartic acid was found in the SDS-insoluble fraction but was absent in muramidase-solubilized material. Comparison of Asp content in total and muramidase-insoluble fractions indicated that the latter accounted for 10% of total SDS-insoluble material. Incidentally, muramidase-undigested material was pronase and amylase resistant. Treatment with both enzymes is part of the standard murein purification procedure (22, 23).

Murein from *T. thermophilus* HB8 has a low reducing sugar content. Samples of murein from *T. thermophilus* HB8 and *E. coli* (nonreducing murein [23]) were subjected to the Park-Johnson test as modified by Ghuysen et al. (21). As positive controls, samples of both mureins were digested with muramidase to generate reducing muropeptides before the colorimetric assay. The results were similar for both mureins, indicating very low reducing sugar contents, 0.5 to 0.9% and 0.9 to 1.1% of total murein sugars for *T. thermophilus* and *E. coli*, respectively. It is interesting to note that the negative result for *T. thermophilus* indicates the absence of reducing sugars in the muramidase-resistant fraction copurified with murein.

Galactosylation of murein from *T. thermophilus* HB8. Milk galactosyltransferase is able to catalyze the transfer of a galactosyl residue from UDP-galactose to the OH at position 4 of GlcNAc (15). The molar ratio of diamino acid to bound galactose gives the number of disaccharide units per glycan chain (3, 52). Murein from *E. coli* was used as a reference because the mean length of glycan chains can be estimated directly by HPLC analysis to calibrate this method (23).

Samples of *T. thermophilus* and *E. coli* murein incorporated [^{3}H]galactose to similar extents. Murein from *T. thermophilus* incorporated $(7.2 \pm 0.32) \times 10^6$ dpm/μmol of Orn, while $(8.8 \pm 0.28) \times 10^6$ dpm/μmol of diaminopimelic acid was incorporated into *E. coli* murein (values ± standard errors). The corresponding values for the diamino acid-to-galactose molar ratio, i.e., disaccharide units per glycan chain, were 30 and 25 for *T. thermophilus* and *E. coli*, respectively. The value for *E. coli* was in good agreement with the HPLC determination: 22 disaccharide units per glycan chain, indicating a high level of efficiency of the labeling reaction.

HPLC analysis of muramidase-digested murein from *T. thermophilus* HB8. Muramidase digests of *T. thermophilus* murein were fractionated by HPLC as described previously for *E. coli* murein (22, 23, 44). Optimization experiments indicated that a longer time under final elution conditions was required to ensure the detection of some late-eluting components. The elution pattern was completely unrelated to the profile for *E. coli* murein treated likewise (Fig. 1). Assuming that most peaks would correspond to authentic muropeptides, murein from *T. thermophilus* looked more complex than that from *E. coli*. The more abundant components (Fig. 1, numbered peaks and peaks A to E) appeared as well-resolved peaks in the elution profile for *T. thermophilus*. The set of numbered components accounted for 85% of the total integrated peak areas.

Effects of pronase and alkali treatments on muropeptide elution pattern of *T. thermophilus* HB8 murein. Murein-bound lipoproteins are a common feature of the cell wall in gram-negative bacteria (6, 48). The omission of pronase treatment in the purification procedure leads to the obtention of murein with intact bound protein. Comparison of HPLC elution profiles for muramidase digests of pronase-treated and untreated samples permits the identification of the protein-anchoring muropeptides. The omission of pronase treatment had no detectable effect on the HPLC elution pattern of *T. thermophilus* muropeptides, suggesting the absence of murein-bound proteins. Furthermore, proteins could not be detected by electrophoretic analysis of muramidase-digested, pronase-untreated murein samples (data not shown).

The peculiar amino acid composition of *T. thermophilus* murein (Table 1) (42, 53), similar to those of some gram-positive bacteria, made us speculate on the presence of teichoic acids. To investigate this possible presence, a sample of murein was treated with 0.1 N NaOH for 2 h at room temperature, prior to muramidase digestion and HPLC analysis. Alkali treatment causes hydrolysis of the teichoic acid-murein linking unit, generating muropeptides with a MurNAc-modified residue which should be detectable as new or modified peaks in the HPLC elution pattern (26). However, no differences between control and alkali-treated samples were detected.

Composition of murein components in *T. thermophilus* HB8. Major components of murein (Fig. 1B, numbered peaks and peaks x and y) were purified and desalted by HPLC. Samples of each fraction were subjected to acid hydrolysis and amino acid analysis (Table 1). All numbered components in Fig. 1B contained Ala, Glu, Orn, and (with the exception of peak 1) Gly. Glu and Orn were always present in essentially equimolar amounts, while the proportions for Ala and Gly were widely variable. Glucosamine and muramic acid were found in all samples; however, the method used was not appropriate for

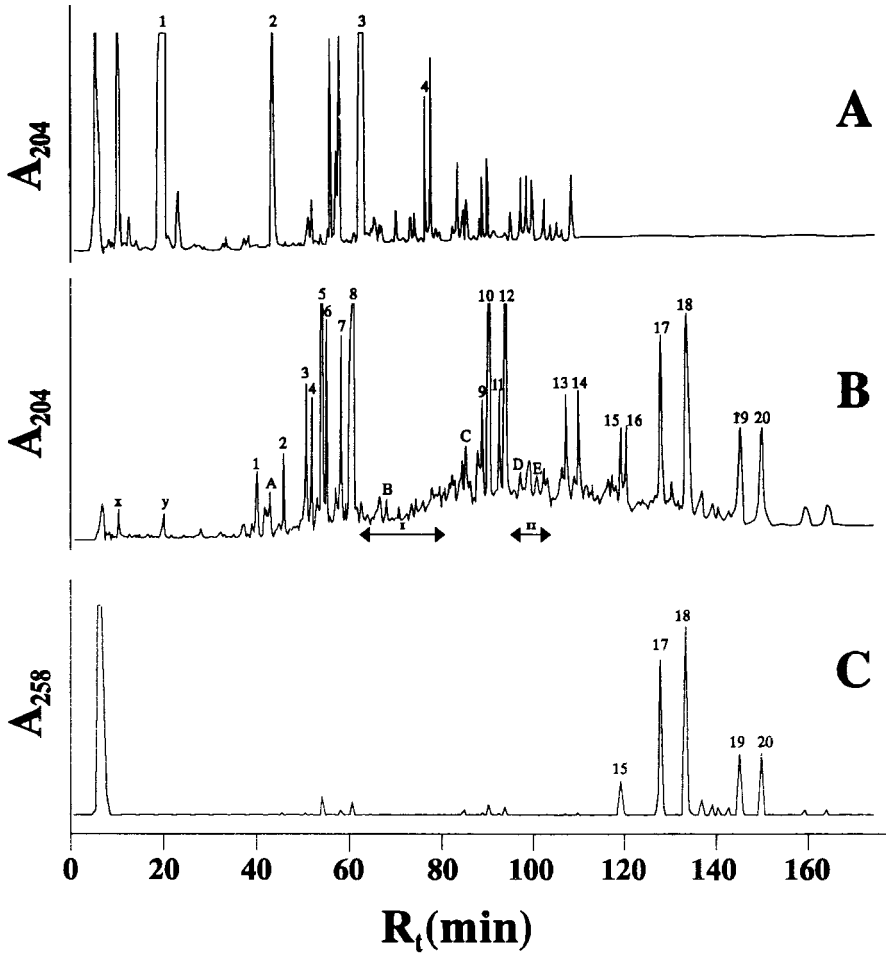

FIG. 1. Analysis of murein composition by HPLC. Samples of murein from *E. coli* (A) and from *T. thermophilus* HB8 (B and C) were subjected to HPLC analysis, and the A_{204}s (A and B) and A_{258} (C) of the eluates were monitored. (A) Muropeptides of *E. coli*: peak 1, GlcNAc–MurNAc–L-Ala–D-Glu–*m*-diaminopimelate–D-Ala; peak 2, GlcNAc–MurNAc–L-Ala–D-Glu–*m*-diaminopimelate–L-Lys–L-Arg; peak 3, bis(GlcNAc–MurNAc–L-Ala–D-Glu–*m*-diaminopimelate–D-Ala); peak 4, tris (GlcNAc–MurNAc–L-Ala–D-Glu–*m*-diaminopimelate–D-Ala) (22, 23, 48). (B and C) Numbers and letters identify the components of *T. thermophilus* murein and correspond between the two panels.

the quantification of amino sugars. No other OPA-reacting compounds were detected in the samples. Peaks x and y (ca. 2% of the total integrated area) rendered only traces of OPA-reacting compounds that, except for Glu, could not be identified.

Minor components could not be individually analyzed. However, series of minor peaks were collected together (Fig. 1B, pools I and II) and the mixtures were subjected to amino acid analysis. The only amino acids and amino sugars detected in the pooled fractions were the same as those found in the major components. These results indicate that the major murein components, and a substantial number of the minor ones, are genuine muropeptides.

In muropeptides, the amino acids with free NH_2 groups are the potential acceptors for the transpeptidation reaction responsible for murein cross-linking. To identify the residues with free NH_2 groups, samples of purified muropeptides were subjected to dinitrophenylation and amino acid analysis as described above. The results shown in Table 1 clearly indicate the presence of free NH_2 groups in either Orn (peaks 1 and 3) or Gly (peaks 2 to 11 and 16). No significant variations (<15%) were detected for muropeptides 12 to 15 and 17 to 20. The facts that in most muropeptides none of the NH_2 groups of Orn was amenable to dinitrophenylation and the concomitant presence of free NH_2 groups on Gly suggest polyglycine-mediated cross-linking, which is common for gram-positive bacteria (53). The apparent absence of free NH_2 groups in some muropeptides suggests an oligomeric nature. Cross-linking could reduce the proportion of NH_2-free to acylated amino acid to below detection level. The blockade of free NH_2 by a non-OPA-reacting compound would be a likely alternative of an absence of free NH_2 groups.

Identification of muropeptides with D-Ala–D-Ala C-terminal dipeptides. Muropeptides with the D-Ala–D-Ala dipeptide interact strongly with vancomycin (15, 16). Muramidase-digested murein was subjected to affinity chromatography on vancomycin-Sepharose, and the retained muropeptides were subsequently identified by HPLC. The results are summarized in Table 1. Murein of *T. thermophilus* was rich in muropeptides containing D-Ala–D-Ala (42.6% of the total integrated area). Interestingly, preservation of the D-Ala–D-Ala dipeptide was not restricted to any particular class of muropeptides.

Determination of relative molecular masses of muropeptides from *T. thermophilus* HB8 by PD MS. The determination of the precise molecular masses of the different muropeptides was crucial to define their structures. Muropeptides were an-

TABLE 1. Compositions of native and dinitrophenylated murein components

Component[a]	RT (min)	Composition[b]							Vancomycin binding
		Native[c]			Dinitrophenylated				
		Orn	Ala	Gly	Glu	Orn	Ala	Gly	
1	39.2	0.8	2.2	0	1	0	2.1	0	−
2	44.9	1.0	0.9	2.6	1	0.7	0.8	1.3	−
3	49.8	1.1	1.5	0.3	1	0.3	1.9	0	+
4	50.9	0.9	1.7	1.9	1	0.8	1.8	1.1	−
5	53.2	1.0	2.0	1.6	1	1.0	2.0	1.0	−
6	53.7	0.9	1.9	3.3	1	0.8	1.7	1.7	−
7	57.3	0.9	2.8	0.7	1	1.1	3.0	0	+
8	59.8	1.2	3.2	2.4	1	0.9	2.7	0.9	+
9	88.7	1.1	2.2	1.9	1	1.0	2.2	1.2	−
10	89.6	1.0	2.1	2.2	1	0.9	2.0	1.3	−
11	92.2	0.9	2.3	1.4	1	0.9	2.5	1.0	+
12	93.3	1.0	2.4	1.7	1	1.0	2.6	1.4	+
13	107.0	0.9	1.9	1.8	1	0.9	1.5	1.4	−
14	108.7	1.1	2.2	2.0	1	1.1	2.5	1.9	+
15	119.4	0.8	2.2	1.5	1	0.8	1.6	1.3	+
16	120.5	0.8	2.2	1.7	1	0.7	2.4	1.3	+
17	126.0	0.8	1.9	1.4	1	1.2	1.9	1.3	−
18	133.8	0.9	2.6	0.7	1	0.8	3.0	1.0	+
19	145.8	1.1	2.1	1.3	1	0.9	1.7	1.2	−
20	150.7	0.8	2.3	1.4	1	0.9	2.3	1.5	−
Pool I	60 to 80	1.0	1.9	1.3	ND[d]	ND	ND	ND	ND
Pool II	95 to 105	0.7	1.7	0.8	ND	ND	ND	ND	ND

[a] Components are numbered as indicated in Fig. 1.
[b] Relative to glutamic acid.
[c] All native components were positive for Glc and Mur, relative to glutamic acid.
[d] ND, not done.

alyzed by ^{252}Cf time-of-flight PDMS in both the positive and negative ion modes (1, 11). The results of the analyses are presented in Table 2. The spectra of a series of representative muropeptides, including monomers, dimers, and trimers, are shown in Fig. 2. The PD MS analyses revealed the presence of two muropeptides each in peaks 3, 10, 15, 17, and 19. Each component was designated with the number of the peak plus a or b for the muropeptide of lower or higher *m/z*, respectively. A theoretical composition for each muropeptide was deduced from the experimental *m/z* values and the analytical data in Table 1. Amino sugars were supposed to be *N*-acetylated as is the rule for mureins (9, 14, 20, 23, 46, 48, 53, 58). The experimental *m/z* values are compared in Table 2 with the values calculated for each muropeptide according to the corresponding theoretical composition.

The *m/z* values for components 1 to 14 were consistent with a series of muropeptides based on a common backbone of GlcNAc-MurNAc-Ala-Glu-Orn, with a variable number of Ala and/or Gly residues bound to the α-carboxyl and δ-amino groups of Orn. The *m/z* values identify muropeptides 1 to 8 as monomers, 9 to 12 as cross-linked dimers, and 13 and 14 as cross-linked trimers.

On the contrary, the *m/z* values for the muropeptides numbered 15 and greater did not fit with any integer number combination of the detected components. However, it was possible to deduce a series of best-fitting likely structures compatible with the analytical data presented in Table 1 and with the backbone proposed for muropeptides 1 to 14. Comparison of the measured and calculated *m/z* values for these muropeptides revealed two groups of compounds; the first group comprised muropeptides 15b and 16, and the second group comprised muropeptides 15a and 17a to 20.

Muropeptides 15b and 16 had the same compositions as muropeptides 11 and 12, respectively, but each with a mass defect of 20.5 Da (Tables 1 and 2). The difference in mass is the one expected (20.03 Da) for the substitution of a MurNAc residue by (1→6)anhydro-MurNAc. It is important to notice that MurNAc in muropeptides is reduced with NaH_4B to *N*-acetylmuramitol, increasing the mass of the muropeptide by 2 Da per MurNAc residue. However, (1→6)anhydro-MurNAc is not susceptible to NaH_4B reduction. This explains why the expected defect in mass was 20.03 Da instead of the 18.02 Da accounted for by the loss of a water molecule. Muropeptides with (1→6)anhydro-MurNAc (anhydro muropeptides) are normal components of murein in *E. coli* and other bacteria (23, 48). Anhydro muropeptides occupy the 1-terminal positions of the glycan chains, explaining the absence of reducing sugars.

The second group of muropeptides with abnormal *m/z* values (15a and 17a to 20) had in common a mass excess of 118 Da over the calculated values for the theoretical best-fit combinations. As far as the amino sugar and amino acid composition are concerned, muropeptides 17a to 20 had equivalents with the expected molecular masses (17a, 3a; 17b, 4; 18, 7; 19a, 9; 19b, 10a; 20, 11). This suggests that the components with the 118-Da mass excess form a family of muropeptides bearing a common substituent (*X*) not detected before. A very similar situation led to the discovery of *N*-acetylputrescine-modified muropeptides in murein from cyanelles of *Cyanophora paradoxa* (46). The putative modified muropeptides, which apparently included both monomers (15a and 17a to 18) and cross-linked dimers (19a to 20), accounted for a substantial fraction of total muropeptides (23.2% of the integrated area; Fig. 1B).

Determination of structure of muropeptides 8 and 18 by ESI with tandem MS. Muropeptide 8 was the best candidate to represent the basic muropeptide for *T. thermophilus* murein. It is a monomer and has the D-Ala–D-Ala terminal dipeptide, two Gly residues (one of them amenable to dinitrophenylation), and an acylated δ-amino group of Orn, and relative molecular mass

TABLE 2. Calculated and measured *m/z* values for protonated and deprotonated molecular ions of major muropeptides

Muropeptide[a]	Ion	*m/z*		Δ*m* (Da)[b]	Error (%)[c]	Muropeptide composition					
		Calculated	Measured			Glc[d]	Mur[e]	Glu	Orn	Ala	Gly
1	$[M + H]^+$	884.91	885.2	0.29	0.03	1	1	1	1	2	0
	$[M - H]^-$	882.90	881.2	−1.70	−0.19						
2	$[M + H]^+$	984.99	985.5	0.51	0.05	1	1	1	1	1	3
	$[M - H]^-$	982.98	983.0	0.02	0.00						
3a	$[M + H]^+$	941.97	942.4	0.43	0.05	1	1	1	1	2	1
	$[M - H]^-$	939.95	937.1	−2.85	−0.30						
3b	$[M - H]^+$	955.99	956.5	0.51	0.05	1	1	1	1	3	0
	$[M - H]^-$	953.98	953.4	−0.58	−0.06						
4	$[M + H]^+$	999.02	998.9	−0.12	−0.01	1	1	1	1	2	2
	$[M - H]^-$	997.00	996.7	−0.30	−0.03						
5	$[M + H]^+$	999.02	999.7	0.68	0.07	1	1	1	1	2	2
	$[M - H]^-$	997.00	996.7	−0.30	−0.03						
6	$[M + H]^+$	1,056.07	1,056.0	−0.07	−0.01	1	1	1	1	2	3
	$[M - H]^-$	1,054.05	1,053.8	−0.25	−0.02						
7	$[M + H]^+$	1,013.04	1,013.1	0.06	0.01	1	1	1	1	3	1
	$[M - H]^-$	1,011.03	1,010.4	−0.63	−0.06						
8	$[M + H]^+$	1,070.10	1,070.4	0.30	0.03	1	1	1	1	3	2
	$[M - H]^-$	1,068.08	1,067.5	−0.58	−0.05						
9	$[M + H]^+$	1,921.96	1,921.3	−0.66	−0.03	2	2	2	2	4	3
	$[M - H]^-$	1,919.95	1,916.6	−3.34	−0.17						
10a	$[M + H]^+$	1,979.01	1,977.6	−1.41	−0.07	2	2	2	2	4	4
	$[M - H]^-$	1,977.00	1,973.9	−3.10	−0.16						
10b	$[M + H]^+$	2,036.07	2,033.4	−2.66	−0.13	2	2	2	2	4	5
	$[M - H]^-$	2,034.05	2,033.2	−0.85	−0.04						
11	$[M + H]^+$	1,993.04	1,991.5	−1.54	−0.08	2	2	2	2	5	3
	$[M - H]^-$	1,991.02	1,986.7	−4.33	−0.21						
12	$[M + H]^+$	2,050.09	2,049.0	−1.09	−0.05	2	2	2	2	5	4
	$[M - H]^-$	2,048.07	2,046.9	−1.17	−0.06						
13	$[M + H]^+$	2,959.00	2,958.4	−0.60	−0.02	3	3	3	3	6	6
	$[M - H]^-$	2,956.99	2,956.6	−0.39	−0.01						
14	$[M + H]^+$	3,030.09	3,028.2	−1.89	−0.06	3	3	3	3	7	6
	$[M - H]^-$	3,028.07	3,023.1	−4.97	−0.16						
15a	$[M + H]^+$	**927.97**[f]	1,046.3	**118.03**[f]		1	1	1	1	1	2
	$[M - H]^-$	**925.96**	1,043.0	**117.04**							
15b	$[M + H]^+$	**1,993.04**	1,972.5	**−20.54**		2	2	2	2	5	3
	$[M - H]^-$	**1,991.02**	1,968.3	**−22.72**							
16	$[M + H]^+$	**2,050.09**	2,029.4	**−20.69**		2	2	2	2	5	4
	$[M - H]^-$	**2,048.07**	2,027.9	**−20.17**							
17a	$[M + H]^+$	**941.97**	1,060.3	**118.33**		1	1	1	1	2	1
	$[M - H]^-$	**939.95**	1,056.9	**116.95**							
17b	$[M + H]^+$	**999.02**	1,116.8	**117.78**		1	1	1	1	2	2
	$[M - H]^-$	**997.00**	1,113.7	**116.70**							
18	$[M + H]^+$	**1,013.04**	1,131.2	**118.16**		1	1	1	1	3	1
	$[M - H]^-$	**1,011.03**	1,127.3	**116.27**							

Continued on following page

TABLE 2—*Continued*

Muropeptide[a]	Ion	*m/z*		Δm (Da)[b]	Error (%)[c]	Muropeptide composition					
		Calculated	Measured			Glc[d]	Mur[e]	Glu	Orn	Ala	Gly
19a	$[M+H]^+$	**1,921.96**	2,038.6	**116.64**		2	2	2	2	4	3
	$[M-H]^-$	**1,919.95**	2,034.0	**114.05**							
19b	$[M+H]^+$	**1,979.01**	2,096.8	**117.79**		2	2	2	2	4	4
	$[M-H]^-$	**1,977.00**	2,090.9	**113.90**							
20	$[M+H]^+$	**1,993.04**	2,110.7	**117.66**		2	2	2	2	5	3
	$[M-H]^-$	**1,991.02**	2,109.2	**118.18**							

[a] Muropeptides are numbered as indicated in Fig. 1.
[b] Difference between measured and calculated protonated or deprotonated molecular mass values.
[c] Calculated as [(measured mass − calculated mass)/calculated mass] × 100.
[d] Glc, *N*-acetylglucosamine.
[e] Mur, *N*-acetylmuramitol.
[f] Boldface characters denote *m/z* values calculated as the most likely combinations of the listed components which nevertheless deviate largely from the observed values.

was determined by PD MS with good mass accuracy (Tables 1 and 2). Muropeptide 18 was selected among the *X*-modified muropeptides because it was expected to be closely related to muropeptide 8. Muropeptide 18 had one *X* and one Gly instead of two Gly residues. No dinitrophenylation-susceptible groups were detected in muropeptide 18, indicating acylation of the remaining Gly residue. It was likely that muropeptides 8 and 18 were identical except for the substitution of the N-terminal Gly in muropeptide 8 by a residue of *X* in muropeptide 18.

Determination of the molecular weight of muropeptides 8 and 18 by positive ion ESI MS at a low sampling-orifice potential revealed protonated molecular ions at *m/z* 1,069.5 and 1,130.4, respectively. The values obtained were consistent with those measured by PD MS (Table 2). In addition to the single-charge molecular ions, double-charge $[M + 2H]^{2+}$ ions at *m/z* 535.3 and 565.8 were present in the ESI mass spectra of muropeptides 8 and 18, respectively. Only a few structurally relevant fragment ions were found. For both muropeptides, monosaccharide related fragment ions were found. For both muropeptides, monosaccharide related fragment ions were observed at *m/z* 204, corresponding to the oxonium ion of the terminal GlcNAc moiety (2, 46). Furthermore, in the ESI mass spectrum of muropeptide 8 a fragment ion arising from the loss of GlcNAc from the $[M + H]^+$ ion was detected at *m/z* 866. Muropeptide 18 exhibited a similar behavior. Unfortunately, ESI mass spectra of muropeptide 18 at increasing sampling-orifice potentials did not reveal additional information concerning the location or the nature of compound *X*.

To further characterize muropeptides 8 and 18, both were analyzed by CID MS, the most powerful tool for the structural analysis of muropeptides (2, 27, 28, 36, 46, 58). Low-energy CID of the single-charged positive molecular ion of muropeptide 18 (*m/z* 1,130.4) yielded a large number of product ions as shown in Fig. 3 and 4. Product ions associated with the reduced disaccharide moiety, a series of peptide backbone fragment ions, and internal fragment ions were generated. Following the notation of Domon and Costello (17), glycosidic fragment ions of the types B_1 and Y_2 were detected at *m/z* 204 and *m/z* 927. Generation of the latter abundant product ion was accompanied by the loss of one and two water molecules (*m/z* 909 and *m/z* 891). The ion at *m/z* 650 represents the loss of the complete carbohydrate moiety (GlcNAc-MurNAc) from the $[M + H]^+$ ion. This observation gave the first clear evidence that the modification must be located at the peptide moiety. The *m/z* 650 product ion further dissociated to *m/z* 579 and *m/z* 450 by the consecutive loss of the Ala and Glu residues, which all represent type y_n product ions in accordance with the peptide fragment ion nomenclature of Biemann (5). In addition, low-intensity type b product ions were observed at *m/z* 1,112 ($[M + H - H_2O]^+$), *m/z* 1,041, and *m/z* 970, the last two being generated by the sequential loss of the C-terminal Ala residues. From these type b fragment ions, further intense ions arise at *m/z* 909, *m/z* 838, and *m/z* 767, corresponding to the loss of the GlcNAc moiety. These ions then lose one (*m/z* 891, *m/z* 820, and *m/z* 749) and two (*m/z* 873, *m/z* 802, and *m/z* 731) water molecules, yielding relatively intense product ions. The observed fragmentation pattern indicated that the modification must be located on the Orn residue and confirmed that the basic amino acid sequence was Ala-Glu-Orn-Ala-Ala (Fig. 4). A second series of peptide backbone product ions, which are directly related to internal fragment ions, were observed at *m/z* 490, *m/z* 419 (the most abundant product ion), and *m/z* 244, corresponding to $[Glu\text{-}Orn(Gly\text{-}X)\text{-}Ala\text{-}CO]^+$, $[Glu\text{-}Orn(Gly\text{-}X)\text{-}CO]^+$, and $[Glu\text{-}Orn\text{-}CO]^+$, respectively (Fig. 4, inset). Based on the mass difference of 175 Da between the internal fragment ions *m/z* 419 and *m/z* 244, the modification in muropeptide 18 can be unambiguously located at the side chain attached to the δ-NH_2 group of Orn. Amino acid analysis of muropeptide 18 indicated the presence of one Gly residue linked to the δ-NH_2 group of Orn. Unfortunately, in the low-energy CID spectrum of muropeptide 18, no product ions which could define the nature of *X* were detected. The CID spectrum of muropeptide 8 was in all respects consistent with that discussed for muropeptide 18 (data not shown). The fragmentation pattern confirms acylation of the δ-NH_2 group of Orn by Gly-Gly (Fig. 4, inset), but as for muropeptide 18, fragments derived from the side chain attached to Orn could not be detected. A more detailed discussion of the CID spectra will be published elsewhere.

Identification of phenylacetic acid as compound *X*. Hydrolysis of muropeptide 18 released Gly and should therefore release *X*. The reaction occurs with the capture of a water molecule; therefore, the molecular mass of free *X* must be 136 Da. As *X* is acylating the Gly residue, it should have a chemical group able to react with a primary amine. The lack of reactivity with OPA indicated the absence of primary amino groups. Compound *X* conferred a more-hydrophobic character to the muropeptides, as indicated by the higher retention times in reversed-phase HPLC. Treatment of modified muropeptides

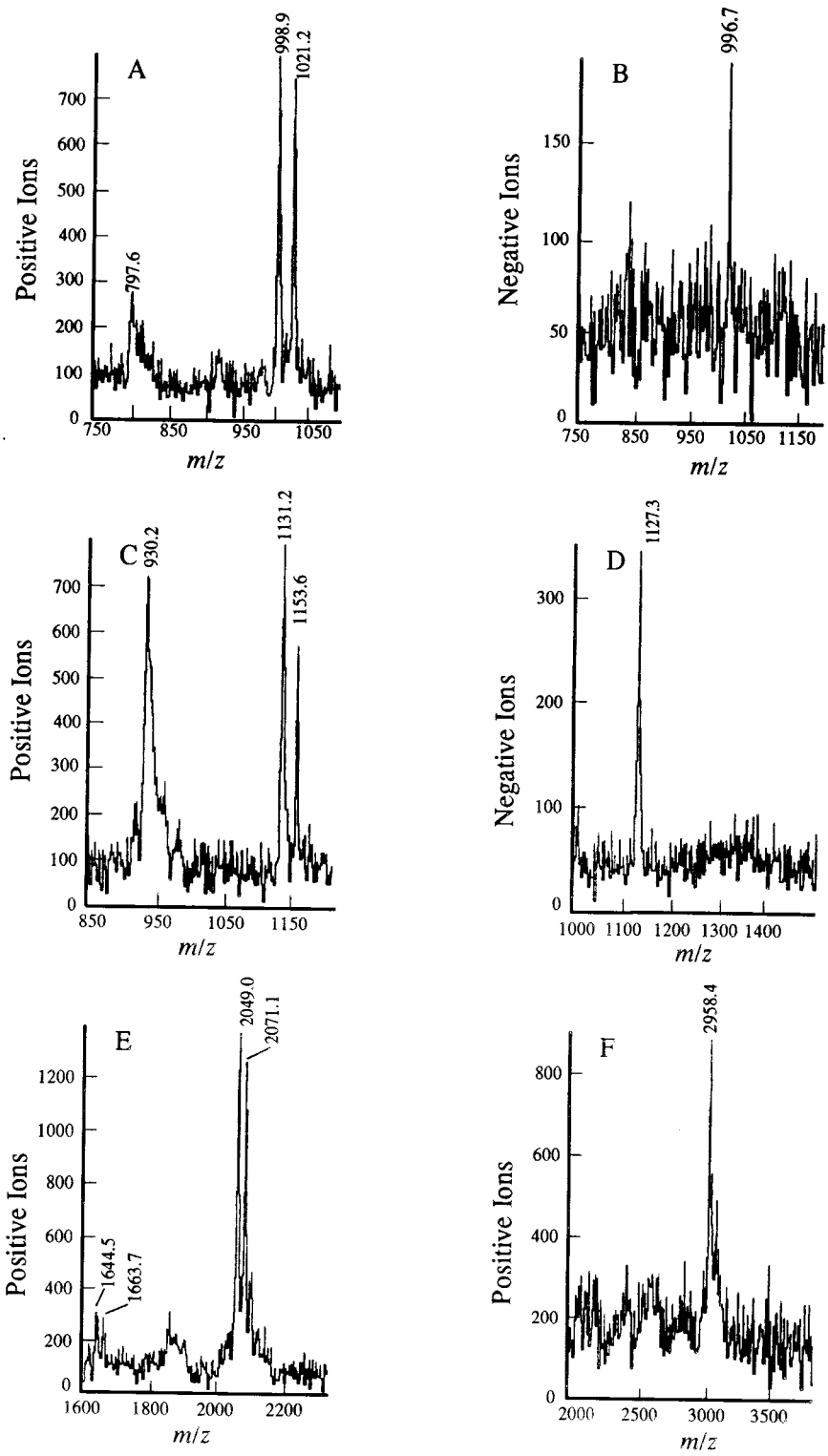

FIG. 2. PD MS spectra of selected muropeptides from *T. thermophilus*. Positive (A, C, E, and F) and negative (B and D) ion mode spectra of muropeptides 4 (A and B), 18 (C and D), 12 (E), and 13 (F). Peaks at *m/z* 998.9 (A), 1,131.2 (C), 2,049.0 (E), and 2,958.4 (F) corresponded to the $[M + H]^+$ molecular ions of the respective muropeptides. Peaks at *m/z* 996.7 (B) and 1,127.3 (D) corresponded to the $[M - H]^-$ molecular ions of the respective muropeptides. Peaks at *m/z* 1,021.2 (A), 1,153.6 (C), and 2,071.1 (E) corresponded to the $[M + Na]^+$ molecular ions of the respective muropeptide. Peaks at *m/z* 797.6 and 930.2 (A and C, respectively) corresponded to $[M - GlcNAc + H]^+$ molecular ions generated by fragmentation of the respective muropeptides. Similarly, the peak at *m/z* 1,644.5 (E) corresponded to $[M - 2GlcNAc + H]^+$ generated by fragmentation of the dimeric muropeptide 12 (46).

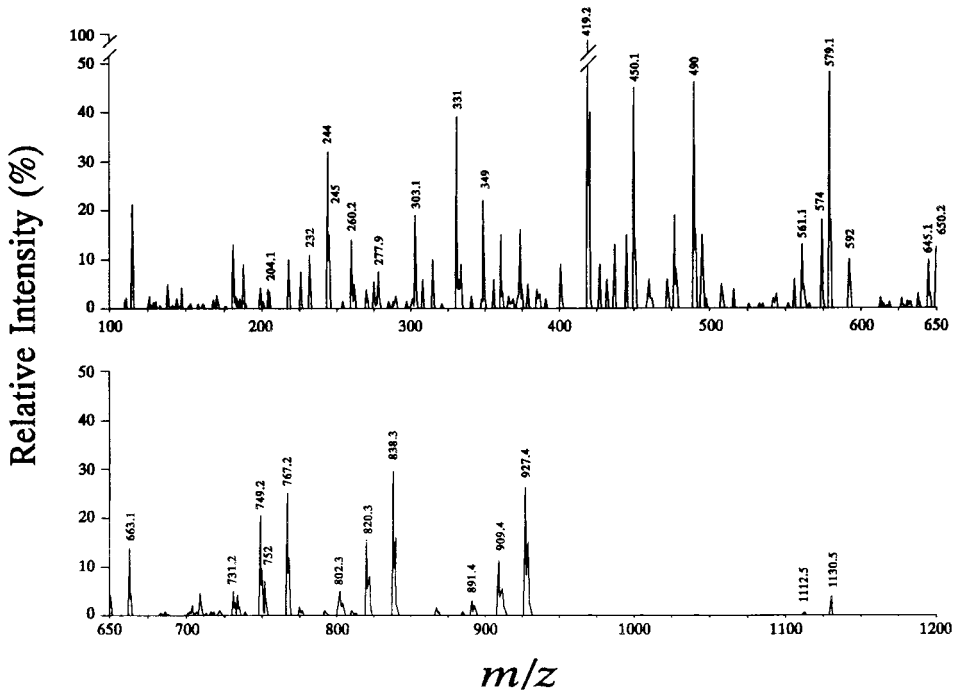

FIG. 3. CID MS spectrum for muropeptide 18 of *T. thermophilus*. The spectrum was obtained as indicated in Materials and Methods. Key fragments are highlighted by inclusion of the respective *m/z* values. The fragmentation pattern is interpreted in Fig. 4.

with oxidative agents (H_2O_2 [10 volumes], 10 min) had no effect on their chromatographic properties, indicating the absence of reduced sulfur. Possible candidates comprised aliphatic and aromatic compounds. The A_{258}s of modified but not of normal muropeptides indicated an aromatic nature for *X* (Fig. 1C). Only phenylacetic and methylbenzoic acids fulfilled the characteristics of compound X. Furthermore, a compound with the expected A_{258} was clearly detected in HCl hydroly-

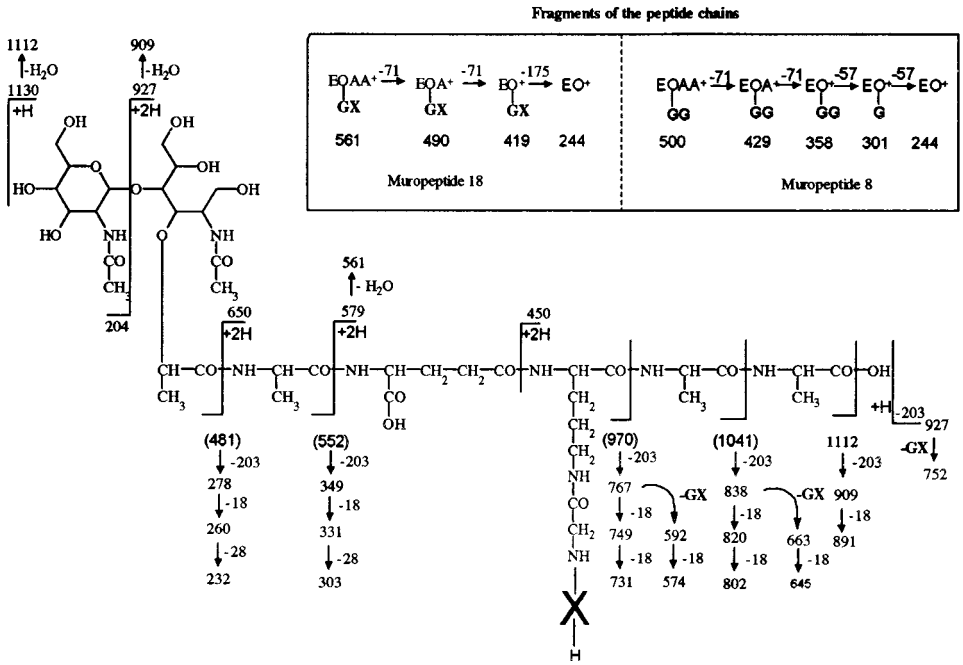

FIG. 4. Schematic representation of the CID MS fragmentation patterns for muropeptides 18 and 8. The fragments shown were positively identified in the corresponding spectra (Fig. 3 for muropeptide 18). In the inset, the main fragments originating from the peptide side chain of muropeptides 8 and 18 are compared. Values in parentheses stand for intermediate fragments which were not detected. X stands for the unknown compound responsible for the mass excess of muropeptide 18.

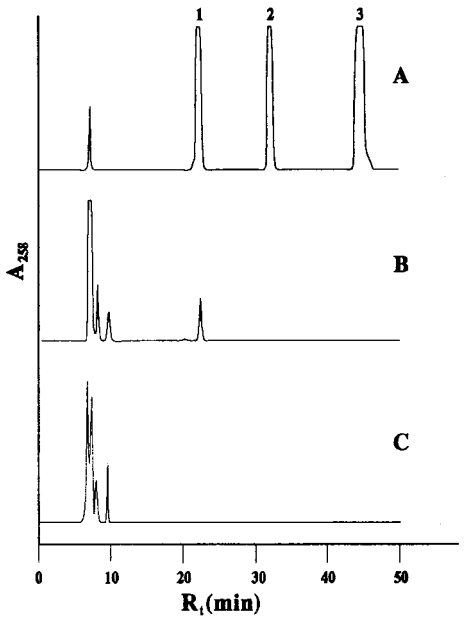

FIG. 5. HPLC analysis of hydrolysates from normal and modified muropeptides of *T. thermophilus*. (A) Phenylacetic acid (peak 1), *o*-methylbenzoic acid (peak 2), and *p*- and *m*-methylbenzoic acid (peak 3) were separated by HPLC in parallel with hydrolysates from modified muropeptide 18 (B) and normal muropeptide 8 (C), and the A_{258}s of the eluates were monitored. Elution conditions were 40 min of isocratic elution in 85% 50 mM sodium phosphate (pH 4.35)–15% acetonitrile followed by a 10-min linear gradient to 75% 50 mM sodium phosphate (pH 4.35)–25% acetonitrile. The flow rate was 0.5 ml/min, and the UV detection was set at 258 nm.

sates from modified but not from normal muropeptides (Fig. 5). Comparison of the HPLC profiles for hydrolysates of modified muropeptides with control runs for phenylacetic acid and the three isomers of methylbenzoic acid showed that *X* had the same RT as the former compound (Fig. 5).

To further characterize *X*, a small sample could be purified by HPLC following HCl hydrolysis of a mixture of modified muropeptides. Aliquots of *X* and authentic phenylacetic acid were subjected to chemical treatments that would convert carboxylic groups into their amide, methyl ester, and methyl acetamide derivatives. The two series of modified compounds obtained were analyzed by HPLC. The results showed in all instances an identical behavior of *X* and phenylacetic acid derivatives. Therefore, we concluded that *X* is indeed phenylacetic acid.

Analysis of minor muropeptides by PD MS. It was possible to obtain small amounts of five minor components of murein which were apparently well-resolved from background peaks (Fig. 1B, lettered peaks). Although the quantities were close to the detection limits, satisfactory PD MS spectra could be obtained, which in the case of peak C revealed the presence of two components (C1 and C2). The measured *m/z* values are shown in Table 3. As not enough material was available for further analyses, we assumed that minor and major muropeptides were built up from the same components. On this basis, it was possible to define theoretical muropeptides whose *m/z* values fitted with the corresponding measured ones and were well within the resolution limits (0.1%) (Table 3). The compositions for muropeptides A, C1, and C2 conformed with the rules observed for the major muropeptides. Component A would correspond to a monomer, while C1 and C2 would correspond to cross-linked dimers. The *m/z* for muropeptide D was 19.5 units lower than the value for muropeptide 7 (Table 2). Actually, this is very close to the mass difference (20.03 Da) associated with the substitution of MurNAc by its (1→6)anhydro derivative, discussed above for muropeptides 15b and 16. Therefore, D was identified as the anhydro form of muropeptide 7.

The theoretical compounds best fitting to the measured *m/z* for components B and E were exceptions to the rule of equimolar proportions for the amino sugars, Glu, and Orn. The composition deduced for component B corresponded to muropeptide 8 (Table 2) with an extra disaccharide unit in the sugar moiety. In fact, the theoretical contribution of a GlcNAc-MurNAc disaccharide would be 478.45 Da, and the difference between measured values for component B and muropeptide 8 was 479.3 Da (Tables 2 and 3). On the contrary, component E would correspond to muropeptide 14, a cross-linked trimer, minus one GlcNAc-*N*-acetylmuramitol moiety. Release of a GlcNAc-*N*-acetylmuramitol group would reduce *m/z* by 480.47 Da. The difference between measured values for E and 14 was −480.3 (Tables 2 and 3). Both B and E could be generated by the action of a MurNAc-L-alanine amidase on murein (30, 55).

Finally, an attempt was made to identify some individual muropeptides in the mixture defined as pool I. To do so, the mixture as such was subjected to PD MS. Negative ion mode spectra could not be obtained because of the very low abundance of the individual components. Nevertheless, three signals of acceptable intensity were detected in the positive ion mode (Table 3). The values indicated theoretical compositions that, from lighter to heavier, would correspond to the dimeric muropeptides 10a, 11, and 12 (Table 2) deprived of one GlcNAc-*N*-acetylmuramitol moiety as proposed for muropeptide E.

Chirality of peptide chain amino acids. The alternation of L and D amino acids is a highly conserved feature of murein peptide side chains (53). Therefore, we expected to find the L enantiomer for the first Ala and Orn and the D enantiomer for Glu. The abilities of a number of muropeptides to bind vancomycin (Table 1) support the hypothesis for the D nature of the Ala residues at positions 4 and 5. To define the chirality of the remaining amino acids, we made use of the specificity of enzymatic reactions. The presence of L-Ala was assayed with L-amino acid oxidase and an HCl hydrolysate of purified muropeptide 5 (Table 2). Muropeptide 5 had 2 mol of Ala per mol of Glu (Tables 1 and 2) and therefore should have equal proportions of both Ala enantiomers if L-Ala were at position 1. A control sample was treated similarly but without enzyme. The results showed that in the enzyme-treated sample, the amount of Ala was 58% of that of the control sample.

The chirality of Orn was assayed with L-ornithine-carbamyltransferase on acid hydrolysates of muramidase-released muropeptides (43). The complete conversion (>95%) of Orn into citrulline indicated the presence of L-Orn in murein.

No appropriate D-enantiomer-specific enzyme was available to assay Glu. Therefore, we selected the L-Glu-specific enzyme L-glutamic decarboxylase (25). Aliquots of the same hydrolysate used for the assay of Orn were treated with L-glutamic decarboxylase. As a negative result was expected, two additional control samples were incubated in parallel. In the first control sample, the activity of the enzyme was confirmed with L-Glu as the substrate. In the second control sample, a known amount of L-Glu (20 μg) was added to an aliquot of the muropeptide hydrolysate (containing 20 μg of Glu). The Glu present in the hydrolysate was not modified by the enzyme, but the control L-Glu was converted to completion. Furthermore, in the mixed sample (L-Glu plus hydrolysate) 48% of total Glu

TABLE 3. Calculated and measured *m/z* values for protonated and deprotonated molecular ions of minor muropeptides

Muropeptide[a]	Ion	*m/z*		Δm (Da)[b]	Error (%)[c]	Muropeptide composition					
		Calculated	Measured			Glc[d]	Mur[e]	Glu	Orn	Ala	Gly
A	$[M + H]^+$	941.97	942.3	0.33	0.04	1	1	1	1	2	1
	$[M - H]^-$	939.95	939.4	−0.55	−0.06						
B	$[M + H]^+$	1,548.55	1,549.9	1.35	0.09	2	2[f]	1	1	3	2
	$[M - H]^-$	1,546.53	1,546.6	0.07	0.00						
C1	$[M + H]^+$	1,907.94	1,907.3	−0.64	−0.03	2	2	2	2	3	4
	$[M - H]^-$	1,905.92	1,905.7	−0.22	−0.01						
C2	$[M + H]^+$	1,964.99	1,964.5	−0.49	−0.03	2	2	2	2	3	5
	$[M - H]^-$	1,962.97	1,963.7	0.73	0.04						
D	$[M + H]^+$	993.01	993.3	0.29	0.03	1	1[g]	1	1	3	1
	$[M - H]^-$	991.00	991.6	0.60	0.06						
E	$[M + H]^+$	2,549.62	2,547.9	−1.72	−0.07	2	2	3	3	7	6
Pool I	$[M + H]^+$	1,498.54	1,498.7	0.16	0.01	1	1	2	2	4	4
Pool I	$[M + H]^+$	1,512.57	1,512.6	0.03	0.00	1	1	2	2	5	3
Pool I	$[M + H]^+$	1,569.62	1,569.9	0.28	0.02	1	1	2	2	5	4

[a] Muropeptides are numbered as indicated in Fig. 1.
[b] Difference between measured and calculated protonated and deprotonated molecular mass values.
[c] Calculated as [(measured mass − calculated mass)/calculated mass] × 100.
[d] Glc, *N*-acetylglucosamine.
[e] Mur, *N*-acetylmuramitol.
[f] *N*-Acetylmuramic acid and *N*-acetylmuramitol (1 mol of each).
[g] (1→6)Anhydro-MurNAc.

was converted into γ-amino butyric acid. We conclude therefore that Glu is in the D form in *T. thermophilus* murein.

Peptide analysis of partial hydrolysates of *T. thermophilus* muropeptides. The high Gly content of the monomeric muropeptides 2 and 6 raised the possibility of heterogeneties in the basic peptide moiety. The 3-to-1 Gly-to-Orn ratio of both muropeptides could be due either to substitution of one D-Ala residue by Gly or to amidation of Glu by Gly, as shown in other instances (53). Therefore, murein and muropeptides 2 and 6 were subjected to partial acid hydrolysis and peptide analysis. Commercial dipeptides were used as standards. Results are shown in Table 4. The detection of Gly-Gly and Ala-Gly indicated that conditions were appropriate for the generation of dipeptides. However, neither Glu-Gly nor Gly-Ala was detected in any sample. The peptide patterns for muropeptides 2 and 6 indicated that a Gly residue was the C-terminal amino acid in both cases.

Structure and sequence of muropeptides from *T. thermophilus* HB8. Information accumulated on the structure of *T. thermophilus* muropeptides is summarized in Fig. 6. Major (numbered) and minor (lettered and pool I) muropeptides should be considered separately because of the difference in the wealth of analytical data as commented before.

The structures proposed in Fig. 6 for the major muropeptides comply with the results from chemical and MS analyses (Tables 1 and 2), as well as with the basic sequence as demonstrated for muropeptides 8 and 18 (Fig. 3 and 4). Compiled data were sufficient to propose defined structures for muropeptides 1, 2, 3a, 3b, 6, 7, 9, 10b, 11, 12, 14, 15a, 17a, 17b, 19a, 19b, and 20.

In the remaining cases, data were not enough to decide among sequence isomers. In muropeptides 4, 5, 10a, and 13, one Gly could occupy either the C-terminal position, as in R–D-Ala–Gly, or the N-terminal one in the diglycine bridge, as in Gly–Gly–(δ)–L-Orn–R′ (see sequences for muropeptides 4 and 5). The ambiguity could be solved for the monomeric muropeptides 4 and 5 by means of partial acid hydrolysis and peptide analysis. Hydrolysis of muropeptide 4 yielded D-Ala–Gly but not Gly-Gly, while the opposite was true for muropeptide 5 (Table 4), supporting the argument for the sequence assignment shown in Fig. 6. Unfortunately, this approach was not suitable for dimers, because in all instances both D-Ala–Gly and Gly-Gly dipeptides would be generated from the peptide bridge R–D-Ala–Gly–Gly–R′. Another ambiguity affected muropeptides 15b and 16. Both are cross-linked dimers with a residue of (1→6)anhydro-*N*-acetylmuramic acid. In neither case was it possible to define whether the anhydro derivative was in the acceptor or in the donor moiety of the dimer.

Sequences for the minor muropeptides were proposed on the basis of their molecular masses and consistency with major

TABLE 4. Peptide analysis of partially hydrolyzed murein and muropeptides[a]

Sample	Dipeptide	
	Gly-Gly	Ala-Gly
Murein	+	+
Muropeptide 2	+	−
Muropeptide 4	−	+
Muropeptide 5	+	−
Muropeptide 6	+	+
Muropeptide 10	+	+

[a] Muropeptides are numbered as indicated in Fig. 1. All samples were negative for Glu-Gly and Gly-Ala.

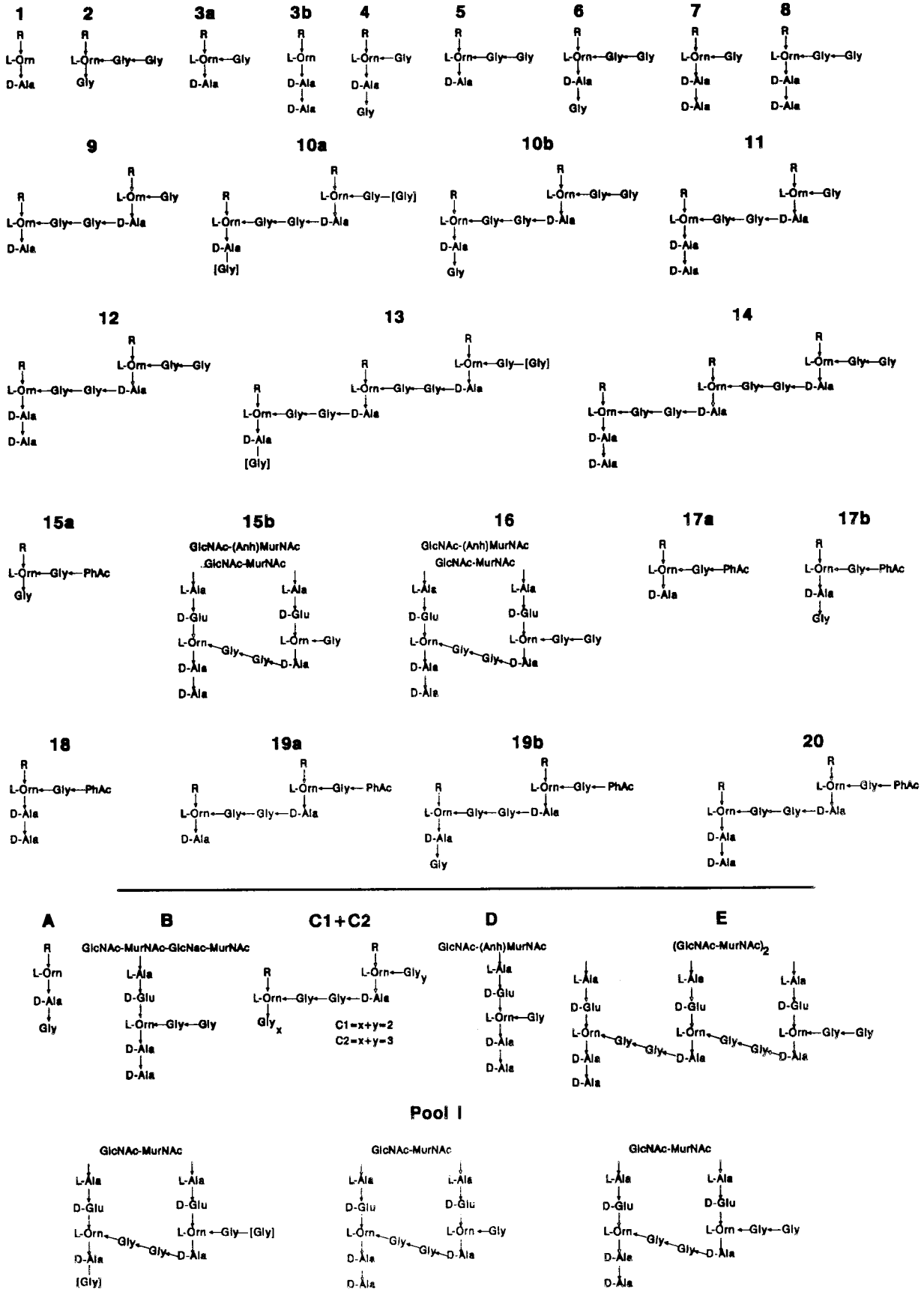

FIG. 6. Primary sequences of *T. thermophilus* muropeptides. Muropeptides are labeled as indicated in Fig. 1. R stands for GlcNAc–MurNAc–L-Ala–D-Glu. Brackets indicate alternative positions for one residue of the amino acid. The precise positions for the glycan moieties in muropeptides 15b and 16, component E, and pool I components could not be established.

TABLE 5. Muropeptide composition of murein from *T. thermophilus* HB8[a]

Muropeptide[b]	Area (%)[c]	Mole (%)[d]
1	1.4	1.9
2	1.7	2.7
3a	1.3	2.3
3b	2.5	4.4
4	1.5	2.5
5	6.9	11.1
6	5.2	7.7
7	3.7	5.9
8	10.3	15.1
9	2.5	2.1
10a	3.8	3.1
10b	3.4	2.7
11	2.6	2.1
12	7.5	5.8
13	2.1	1.2
14	1.1	0.6
15a	0.6	0.8
15b	0.9	0.8
16	1.1	0.9
17a	4.1	5.0
17b	3.6	4.0
18	8.3	9.4
19a	1.8	1.2
19b	1.5	1.0
20	3.3	2.3
A	1.0	1.7
B	0.5	0.4
C	0.4	0.4
D	0.5	0.7
E	0.3	0.2

[a] Structural parameters (calculated from muropeptide molar proportions) were as follows: monomers, 75%; dimers, 23%; trimers, 2%; cross-linkage, 27%; C-terminal dipeptides, D-Ala–D-Ala (48.4%) and D-Ala–Gly (23.9%); phenyl acetate-containing muropeptides, 23.7%.

[b] Muropeptides are numbered as indicated in Fig. 1.

[c] Percentage of total integrated area.

[d] Molar proportions calculated upon correction of integrated area values for the degree of oligomerization, number of amide bonds (22), and phenylacetic acid content.

muropeptides. In the cases of C1 and C2, ambiguity of the positions of some Gly residues could not be resolved. The absence of major muropeptides with Orn or Gly-Gly at the C-terminal position of the peptide chain would suggest that X and Y are 1 for C1 and that X is 1 and Y is 2 for C2. Likewise, in the case of E and the muropeptides in the pool I fraction, the position of the disaccharide moieties could not be defined.

Molar proportions of muropeptides in murein were estimated from the HPLC elution profiles as proposed by Glauner et al. (23). However, for *T. thermophilus* an additional correction was required for phenylacetic acid-containing muropeptides. Comparison of the A_{204}s of known amounts of muropeptides 8 and 18 indicated that the substitution of a Gly by phenylacetic acid increases the A_{204} by a factor of 1.3. When two muropeptides coeluted, the individual abundances were assumed to be proportional to the relative intensities of the respective signals in the PD MS spectra, as a rough approximation.

The results displayed in Table 5 indicated that murein from *T. thermophilus* had a degree of cross-linkage (27%) similar to that for *E. coli* (23, 44, 48). Dimers were the most abundant cross-linked muropeptides, although the proportion of trimers was significant (10% of cross-linked muropeptides). A large proportion (48.4%) of muropeptides conserved the D-Ala–D-Ala terminal dipeptide, and an important fraction (23.9%) had instead D-Ala–Gly as the C-terminal dipeptide. The δ-NH_2 group of Orn was acylated in most muropeptides (92%). The most frequent acylating group was Gly-Gly, but muropeptides with either phenylacetyl-Gly or Gly were both abundant. Phenylacetic acid-containing muropeptides accounted for 23.7% of total muropeptides. Finally, it is interesting to note the absence of muropeptides with Orn as the C-terminal amino acid.

DISCUSSION

The composition and structure of murein from the thermophilic eubacterium *T. thermophilus* HB8 were investigated. The murein purification method devised for *E. coli* could be applied to *T. thermophilus* with minor modifications. The hot-SDS-insoluble fraction obtained consisted of murein and some copurifying additional component(s). The latter could derive from the thick amorphous structure that overlays murein, as visualized by electron microscopy (7, 12). More than 97% of Orn in the murein fraction was solubilized upon muramidase digestion. The omission of major components in the solubilized fraction seems unlikely. However, we cannot rule out the possibility that minor components with important functions could be missed because of experimental limitations. Muropeptides with as low an abundance as 0.1% would still provide a considerable number of, for instance, attachment sites for a macromolecule. The low murein content of *T. thermophilus* HB8 is in agreement with the thin sacculus shown by electron microscopy and with the gram-negative character of *Thermus* spp. (8). On the basis of weight, the amount of murein present in *T. thermophilus* HB8 is one-half the amount of that present in *E. coli*. The small amount of murein could explain the apparent inability of the sacculus to preserve by itself the cell morphology in S-layer-deficient derivatives of *T. thermophilus* HB8 (32).

The separation of muramidase-solubilized fragments by HPLC produced a chromatogram unrelated to those for *E. coli* and other gram-negative bacteria (23, 48, 58). A large number of components were detected. Fortunately, for such a complex mixture the resolution was good enough to permit purification of the more abundant components. Chemical and MS analyses identified the major components as muropeptides. Minor components could not be analyzed individually. However, amino acid analysis of pooled fractions indicated that most minor peaks might also correspond to muropeptides or muropeptide-derived fragments.

Muropeptide 8 apparently represents the basic monomeric subunit. The amino sugar and amino acid sequence demonstrated for this muropeptide was GlcNAc–MurNAc–L-Ala–D-Glu–L-Orn–D-Ala–D-Ala, with a Gly-Gly dipeptide acylating the δ-NH_2 of Orn. Although experimental demonstration was not possible, it seems reasonable to assume a D-Glu–γ–L-Orn arrangement, as, to our knowledge, no exception has been reported (9, 53). Of particular interest was the finding of a family of muropeptides with phenylacetyl-Gly instead of di-Gly acylating the Orn residue. Muropeptide 18 was the modified form of the basic muropeptide 8. The presence of phenylacetic acid in murein has interesting implications which are discussed below.

The muropeptides displayed in Fig. 6 could be understood as being derived from the basic ones (muropeptides 8 and 18) by the activity of the enzymes normally involved in murein metabolism (transpeptidases, endopeptidases, and carboxypeptidases) (29, 51). Cross-linking is apparently effected by di-Gly peptide bridges. Oligoglycine-mediated cross-linking is rather

common among gram-positive bacteria, but it is exceptional for a gram-negative bacterium (53). Both cross-linked dimers and trimers were detected. Higher-order oligomers are possible but were not detected among the major muropeptides. The degree of cross-linkage (27%) was close to the values described for *E. coli* (about 30%) and other gram-negative bacteria (16, 22, 23, 44, 48).

The low proportion of muropeptides with free δ-NH_2-Orn in macromolecular murein suggests complete acylation at the precursor level. Muropeptides with D-Ala–D-Ala or D-Ala–Gly C-terminal dipeptides were both rather abundant (48.4 and 23.9% of total muropeptides, respectively). The dipeptide D-Ala–D-Ala, present in murein precursors, is all-important in murein biosynthesis as the donor group for transpeptidation and subsequent cross-linking (29, 51). However, there is wide disparity in the degree of preservation of the dipeptide in mature murein. In some species (*E. coli* and *Pseudomonas putida*) it is hardly detectable (23, 48), while in others (*Caulobacter crescentus* and *Staphylococcus aureus*) it is retained in a large fraction of muropeptides (14, 35). The variability of this parameter has not been related to any particular property of a bacterium up to now.

Muropeptides with a D-Ala–Gly C-terminal dipeptide were in principle unexpected. Two mechanisms could explain their formation and accumulation: (i) incorporation of Gly instead of D-Ala in the synthesis of D-Ala–D-Ala by D-Ala:D-Ala ligase and (ii) enzymatic cleavage of peptide bridges at the Gly-Gly bond of cross-linked muropeptides. The former alternative has been demonstrated for both gram-positive and gram-negative bacteria (22, 59). The latter would imply the presence of a Gly-Gly endopeptidase similar to lysostaphin (49). None of the alternatives can be discarded at present, and both could coexist for *T. thermophilus*. However, two arguments favor the latter. First, the relative abundance of R–D-Ala–Gly muropeptides (23.9% of total muropeptides) seems too high for enzymatic misincorporation (ca. 4% in *E. coli*) (22, 23). Second, the proportions of R–D-Ala–Gly muropeptides and of muropeptides with a single Gly at the δ-NH_2 of Orn (20.7% of total muropeptides), the other expected product for a Gly-Gly endopeptidase, matched each other. If R–D-Ala–Gly muropeptides were mostly of lytic origin, it would suggest a high turnover of peptide cross-bridges in macromolecular murein. Turnover of peptide cross-bridges has been described for *E. coli* and is believed to be a relevant aspect of postinsertional murein metabolism (24).

Muropeptides 2 and 15a are exceptions to the basic sequence as proposed above. They have in common a Gly at position 4 as the C-terminal amino acid. The only known mechanism that could explain their formation is the lack of specificity for the D-Ala:D-Ala ligase. In this instance, the scarcity of both muropeptides would argue in favor of the idea.

Glycan chains were terminated by nonreducing sugars, as indicated by both the lack of reducing power in total murein and the positive identification of muropeptides with (1→6)anhydro-MurNAc. Galactosylation of the terminal GlcNAc indicated a mean glycan chain length of 30 disaccharide units.

No indications supporting the presence of modified sugar residues were found. Pronase and alkali treatments had no detectable effects on the muropeptide pattern. Therefore, covalent binding of macromolecules to *T. thermophilus* murein seems to be rather restricted, raising the question of how murein and the spatially remote S-layer interact with each other.

The detection of muropeptides with nonequimolar proportions of sugars, Glu, and Orn (B, E, and pool I) was unexpected. In all instances, they were minor, and therefore analytical data were not as complete as for major muropeptides. Nevertheless, the action of an *N*-acetylmuramyl-L-alanine amidase on murein could easily explain the formation of these muropeptides. Amidases are widespread murein hydrolases (30, 55). Therefore, their presence on *T. thermophilus* would not be a particularly rare event.

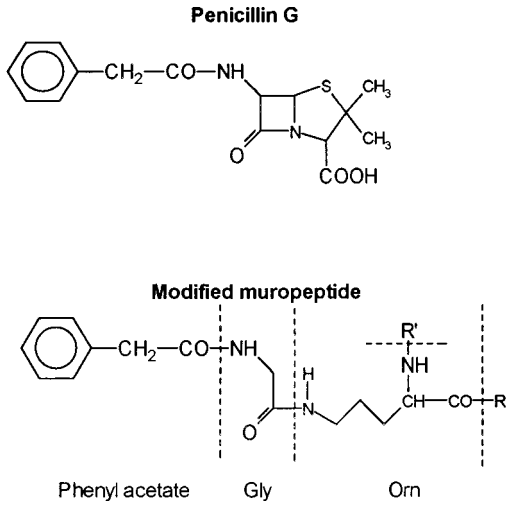

FIG. 7. Structural comparison of benzylpenicillin and phenyl acetate-modified muropeptides.

The more distinctive feature of *T. thermophilus* murein was the presence of muropeptides with phenylacetic acid residues. To our knowledge, this is the first case in which phenylacetic acid is identified as a murein component. Phenylacetic acid substituted for the N-terminal Gly in a considerable proportion of muropeptides (23.7%). Preliminary experiments indicated that the abundance of modified muropeptides is independent of externally added phenylacetic acid, suggesting that it is a regulated phenomenon (results not shown). However, the origin of phenylacetic acid and the level at which incorporation occurs remain unknown. Because phenylacetic acid effectively blocks potential transpeptidation acceptor sites in murein, misregulation could be harmful, even lethal, if a high accumulation were ever to occur. Therefore, awaiting a physiological role for the modified muropeptides seems sensible. The introduction of an aromatic ring in the highly polar murein could be a strategy to facilitate noncovalent interaction with hydrophobic domains of another macromolecule or macromolecular complex in an aqueous environment, for instance the amorphous or S-layers. A second alternative also seems appealing. Phenylacetyl-Gly-δ-Orn has a striking structural similarity to the side chain and part of the β-lactam ring of benzylpenicillin (penicillin G) (Fig. 7). As a matter of fact, this similarity is more extensive than the homology between D-Ala–D-Ala and the β-lactam ring, the basis for the antibiotic action of β-lactams (57). The side substituent of β-lactams strongly conditions the specificity of binding to the penicillin-binding proteins, the enzymes responsible for macromolecular murein biosynthesis (29, 54, 56, 60). Therefore, phenylacetic acid-modified muropeptides could mediate interactions between murein and penicillin-binding proteins that are relevant at the high growth temperature of *T. thermophilus.*

To summarize, the murein layer of *T. thermophilus* HB8 seems to be structurally intermediate between standard gram-positive and gram-negative cell walls. The chemical composition and peptide bridges of this bacterium are typical of gram-

positive bacteria. However, the abundance, degree of cross-linkage, and glycan chain mean length of this bacterium are closer to those of gram-negative bacteria. The presence of phenylacetic acid is a unique feature of *T. thermophilus* murein at present. Work aimed at characterizing murein-copurifying macromolecules, murein-degrading enzymes, and the phenylacetic acid incorporation pathway in *T. thermophilus* is in progress.

ACKNOWLEDGMENTS

We are grateful to H. Kaudewitz (Perkin Elmer, Vatterstetten, Germany) for excellent technical assistance in obtaining the CID spectra. The technical assistance of J. de la Rosa is greatly appreciated.

This work was supported by grant BIO94-0789 from the CICYT and an institutional grant from the Fundación Ramón Areces to M.A.P. and grant 4840 from the Jubilaeumsfond der Oesterreichischen Nationalbank to G.A. Travel money was provided by Acción Integrada Austria-España 22B and the Mixed Committee for Scientific and Technical Cooperation Austria-Spain. J.C.Q. was supported by a fellowship from Residencia de Estudiantes-Ayuntamiento de Madrid, Spain.

REFERENCES

1. **Allmaier, G., M. C. Rodriguez, and E. Pittenauer.** 1992. Optimization of sample deposition for plasma desorption mass spectrometry. Rapid Commun. Mass Spectrom. **6:**284–288.
2. **Allmaier, G., and E. R. Schmid.** 1993. New mass spectrometry methods for peptidoglycan analysis, p. 23–30. *In* M. A. de Pedro, J.-V. Höltje, and W. Löffelhardt (ed.), Bacterial growth and lysis: metabolism and structure of the bacterial sacculus. Plenum Press, New York.
3. **Beachey, E. H., W. Keck, M. A. de Pedro, and U. Schwarz.** 1981. Exoenzymatic activity of transglycosilase isolated from *Escherichia coli*. Eur. J. Biochem. **116:**355–358.
4. **Berquist, P. L., D. R. Love, J. E. Croft, M. B. Steiff, R. M. Daniel, and W. H. Morgan.** 1987. Genetics and potential biotechnological applications of thermophilic and extremely thermophilic microorganisms. Biotechnol. Genet. Eng. Rev. **5:**199–244.
5. **Biemann, K.** 1990. Nomenclature for peptide fragment ions (positive ions). Methods Enzymol. **193:**886–887.
6. **Braun, V., and H. C. Wu.** 1994. Lipoproteins, structure, function, biosynthesis and model for protein export, p. 319–341. *In* J.-M. Ghuysen and R. Hakenbeck (ed.), Bacterial cell wall. Elsevier Science Publisher B.V., Amsterdam.
7. **Brock, T. D.** 1978. Thermophilic microorganisms and life at high temperatures, p. 72–91. Springer-Verlag, New York.
8. **Brock, T. D.** 1984. Genus *Thermus* Brock and Freeze 1969, 295^{AL}, p. 333–337. *In* N. R. Krieg and J. G. Holt (ed.), Bergey's manual of systematic bacteriology, vol. 1. The Williams & Wilkins Co., Baltimore.
9. **Burroughs, M., Y.-S. Chang, D. A. Gage, and E. I. Tuomanen.** 1993. Composition of the peptidoglycan of *Haemophilus influenzae*. J. Biol. Chem. **268:**11594–11598.
10. **Caparrós, M., A. G. Pisabarro, and M. A. de Pedro.** 1992. Effect of D-amino acids on structure and synthesis of peptidoglycan in *Escherichia coli*. J. Bacteriol. **174:**5549–5559.
11. **Caparrós, M., E. Pittenauer, E. R. Schmid, M. A. de Pedro, and G. Allmaier.** 1993. Molecular weight-determination of biosynthetically modified monomeric and oligomeric muropeptides from *Escherichia coli* by plasma desorption mass spectrometry. FEBS Lett. **316:**181–185.
12. **Castón, J. R., J. Berenguer, M. A. de Pedro, and J. L. Carrascosa.** 1993. S-layer protein from *Thermus thermophilus* HB8 assembles into porin-like structure. Mol. Microbiol. **9:**65–75.
13. **Castón, J. R., J. Berenguer, E. Kocsis, and J. L. Carrascosa.** 1994. Three-dimensional structure of different aggregates built up by the S-layer protein of *Thermus thermophilus*. J. Struct. Biol. **113:**164–176.
14. **De Jonge, B. L. M., Y.-S. Chang, D. Gage, and A. Tomasz.** 1992. Peptidoglycan composition of a highly methicillin-resistant *Staphylococcus aureus* strain. J. Biol. Chem. **267:**11248–11254.
15. **de Pedro, M. A., and U. Schwarz.** 1980. Affinity chromatography of murein precursors on vancomycin sepharose. FEMS Microbiol. Lett. **9:**215–217.
16. **de Pedro, M. A., and U. Schwarz.** 1981. Heterogeneity of newly inserted and preexisting murein in the sacculus of *Escherichia coli*. Proc. Natl. Acad. Sci. USA **78:**5856–5860.
17. **Domon, B., and C. E. Costello.** 1988. A systematic nomenclature for carbohydrate fragmentation in FAB-MS/MS spectra of glycoconjugates. Glycoconj. J. **5:**397–409.
18. **Edwards, C.** 1990. Thermophiles, p. 1–32. *In* C. Edwards (ed.), Microbiology of extreme environments. Open University Press, Milton Keynes, United Kingdom.
19. **Faraldo, M. L., M. A. de Pedro, and J. Berenguer.** 1988. Purification, composition and Ca^{2+} binding properties of the monomeric protein of the S-layer of *Thermus thermophilus*. FEBS Lett. **235:**117–121.
20. **García-Bustos, J., and A. Tomasz.** 1987. Structure of the peptide network of pneumococcal peptidoglycan. J. Biol. Chem. **262:**15400–15405.
21. **Ghuysen, J.-M., D. J. Tipper, and J. L. Strominger.** 1966. Enzymes that degrade bacterial cell walls. Methods Enzymol. **8:**685–700.
22. **Glauner, B.** 1988. Separation and quantification of muropeptides with high-performance liquid chromatography. Anal. Biochem. **172:**451–464.
23. **Glauner, B., J.-V. Höltje, and U. Schwarz.** 1988. The composition of the murein of *Escherichia coli*. J. Biol. Chem. **263:**10088–10095.
24. **Goodell, E. W., and U. Schwarz.** 1983. Cleavage and resynthesis of peptide cross-bridges in *Escherichia coli*. J. Bacteriol. **156:**136–140.
25. **Hager, L. P.** 1970. Glutamate decarboxylase (*Escherichia coli*). Methods Enzymol. **XVIIA:**857–863.
26. **Hammond, S. M., P. A. Lambert, and A. N. Rycroft.** 1984. The bacterial cell surface, p. 29–56. Croom Helm, London.
27. **Handwerger, S., M. J. Pucci, K. J. Volk, J. Liu, and M. S. Lee.** 1992. The cytoplasmic peptidoglycan precursor of vancomycin-resistant *Enterococcus faecalis* terminates in lactate. J. Bacteriol. **174:**5982–5984.
28. **Handwerger, S., M. J. Pucci, K. J. Volk, J. Liu, and M. S. Lee.** 1994. Vancomycin-resistant *Leuconostoc mesenteroides* and *Lactobacillus casei* synthesize cytoplasmic peptidoglycan precursors that terminate in lactate. J. Bacteriol. **176:**260–264.
29. **Höltje, J.-V., and U. Schwarz.** 1985. Biosynthesis and growth of the murein sacculus, p. 77–119. *In* N. Nanninga (ed.), Molecular cytology of *E. coli*. Academic Press, London.
30. **Höltje, J.-V., and E. Tuomanen.** 1991. The murein hydrolases of *Escherichia coli* properties, functions and impact on the course of infections in vivo. J. Gen. Microbiol. **137:**441–454.
31. **Kato, K., T. Umemoto, H. Sagawa, and S. Kotani.** 1979. Lanthionine as an essential constitutent of cell wall peptidoglycan of *Fusobacterium nucleatum*. Curr. Microbiol. **3:**147–151.
32. **Lasa, I., J. R. Castón, L. A. Fernández-Herrero, M. A. de Pedro, and J. Berenguer.** 1992. Insertional mutagenesis in the extreme thermophilic eubacteria *Thermus thermophilus* HB8. Mol. Microbiol. **6:**1555–1564.
33. **Lasa, I., M. de Grado, M. A. de Pedro, and J. Berenguer.** 1992. Development of *Thermus-Escherichia* shuttle vectors and their use for expression of the *Clostridium thermocellum celA* gene in *Thermus thermophilus*. J. Bacteriol. **174:**6424–6431.
34. **Lennox, E. S.** 1955. Transduction of linked genetic characters of the host by bacteriophage P1. Virology **1:**190–206.
35. **Markiewicz, Z., B. Glauner, and U. Schwarz.** 1983. Murein structure and lack of DD- and LD-carboxypeptidase activities in *Caulobacter crescentus*. J. Bacteriol. **156:**649–655.
36. **Martin, S. A.** 1988. Mass spectrometry of peptidoglycans, p. 129–145. *In* P. Actor, L. Daneo-Moore, M. L. Higgins, M. R. J. Salton, and G. D. Shockman (ed.), Antibiotic inhibition of bacterial cell surface assembly and function. American Society for Microbiology, Washington, D.C.
37. **Messner, P., and U. B. Sleytr.** 1992. Crystalline bacterial cell-surface layer. Adv. Microb. Physiol. **33:**213–275.
38. **Nakamura, M., and M. E. Jones.** 1970. Ornithine carbamyltransferase (*Streptococcus faecalis*). Methods Enzymol. **XVIIA:**286–297.
39. **Nakano, M., and T. S. Danowski.** 1971. L-Amino acid oxidase (rat kidney). Methods Enzymol. **XVIIB:**601–605.
40. **Oshima, T., and K. Imahori.** 1974. Description of *Thermus thermophilus* (Yoshida and Oshima) comb. nov., a nonsporulating thermophilic bacterium from a Japanese thermal spa. Int. J. Syst. Bacteriol. **24:**102–112.
41. **Pask-Hughes, R. A., and N. Shaw.** 1982. Glycolipids from some extreme thermophilic bacteria belonging to the genus *Thermus*. J. Bacteriol. **149:**54–58.
42. **Pask-Hughes, R. A., and R. A. D. Williams.** 1978. Cell envelope components of strains belonging to the genus *Thermus*. J. Gen. Microbiol. **107:**65–72.
43. **Perkins, H. R., and C. S. Cummins.** 1964. Ornithine and 2,4-diaminobutyric acid as components of the cell walls of plant pathogenic *Corynebacteria*. Nature (London) **201:**1105–1107.
44. **Pisabarro, A. G., M. A. de Pedro, and D. Vázquez.** 1985. Structural modifications in the peptidoglycan of *Escherichia coli* associated with changes in the state of growth of the culture. J. Bacteriol. **161:**238–242.
45. **Pittenauer, E., G. Allmaier, and E. R. Schmid.** 1993. Structure elucidation of peptidoglycan monomers by fast atom bombardment and electrospray ionization tandem-mass spectrometry, p. 39–46. *In* M. A. de Pedro, J.-V. Höltje, and W. Löffelhardt (ed.), Bacterial growth and lysis: metabolism and structure of the bacterial sacculus. Plenum Press, New York.
46. **Pittenauer, E., E. R. Schmid, G. Allmaier, B. Pfanzagl, W. Löffelhardt, C. Quintela-Fernández, M. A. de Pedro, and W. Stanek.** 1993. Structural characterization of the cyanelle peptidoglycan of *Cyanophora paradoxa* by ^{252}Cf plasma desorption mass spectrometry and fast atom bombardment/tandem mass spectrometry. Biol. Mass Spectrom. **22:**524–536.
47. **Prats, R., and M. A. de Pedro.** 1989. Normal growth and division of *Escherichia coli* with a reduced amount of murein. J. Bacteriol. **171:**3740–3745.
48. **Quintela, J. C., M. Caparrós, and M. A. de Pedro.** 1995. Variability of

peptidoglycan structural parameters in Gram-negative bacteria. FEMS Microbiol. Lett. **125:**95–100.
49. **Recsei, P. A., A. D. Gruss, and R. P. Novick.** 1987. Cloning, sequence, and expression of the lysostaphin gene from *Staphylococcus simulans*. Proc. Natl. Acad. Sci. USA **84:**1127–1131.
50. **Roepstorff, P.** 1989. Plasma desorption mass spectrometry of peptides and proteins. Acc. Chem. Res. **22:**421–427.
51. **Rogers, H. J., H. R. Perkins, and J. B. Ward.** 1980. Microbial cell walls and membranes, p. 239–297. Chapman and Hall, London.
52. **Schindler, M., D. Mirelman, and U. Schwarz.** 1976. Quantitative determination of N-acetylglucosamine residues at the non-reducing ends of peptidoglycan chains by enzymic attachment of [^{14}C]-D-galactose. Eur. J. Biochem. **71:**131–134.
53. **Schleifer, K. H., and O. Kandler.** 1972. Peptidoglycan types of bacterial cell walls and their taxonomic implications. Bacteriol. Rev. **36:**407–477.
54. **Selwyn, S.** 1980. The mechanism and range of activity of penicillins and cephalosporins, p. 56–90. *In* S. Selwyn (ed.), The beta-lactam antibiotics: penicillins and cephalosporins in perspective. Hodder and Stoughton, London.
55. **Shockman, G. D., and J.-V. Höltje.** 1994. Microbial peptidoglycan (murein) hydrolases, p. 131–166. *In* J.-M. Ghuysen and R. Hakenbeck (ed.), Bacterial cell wall. Elsevier Science Publisher B.V., Amsterdam.
56. **Spratt, B. G.** 1983. Penicillin-binding proteins and the future of β-lactam antibiotics. J. Gen. Microbiol. **129:**1247–1260.
57. **Tipper, J. A., and J. L. Strominger.** 1965. Mechanism of action of penicillins: a proposal based on their structural similarity to acyl-D-alanyl-D-alanine. Proc. Natl. Acad. Sci. USA **54:**1133–1141.
58. **Tuomanen, E., J. Schwartz, S. Sande, K. Light, and D. Gage.** 1989. Unusual composition of peptidoglycan in *Bordetella pertussis*. J. Biol. Chem. **264:** 11093–11098.
59. **Van Heijenoort, J.** 1994. Biosynthesis of the bacterial peptidoglycan unit, p. 39–71. *In* J.-M. Ghuysen and R. Hakenbeck (ed.), Bacterial cell wall. Elsevier Science Publisher B.V., Amsterdam.
60. **Waxman, D. J., and J. L. Strominger.** 1983. Penicillin-binding proteins and the mechanism of action of β-lactam antibiotics. Annu. Rev. Biochem. **52:** 825–869.
61. **Work, E.** 1957. Reaction of ninhydrin in acid solution with straight-chain amino acids containing two amino groups and its application to the estimation of αε-diaminopimelic acid. Biochemistry **67:**416–423.